

## **Petroleum geochemistry of the Albian-Turonian Sarvak reservoir in one of the oil fields of southwest Iran**

**Milad Zohrevand<sup>1</sup>, Ali Shekarifard<sup>2,3\*</sup>, Vahid Tavakoli<sup>1</sup>**

<sup>1</sup> School of Geology, College of Science, University of Tehran, Tehran, Iran

<sup>2</sup> Oil and Gas Engineering Group, School of Chemical Engineering, College of Engineering, University of Tehran, Tehran, Iran

<sup>3</sup> Institute of Petroleum Engineering (IPE), College of Engineering, University of Tehran, Tehran, Iran

### **Abstract**

Organic geochemical investigations using thin layer chromatography-flame ionization detection (TLC-FID), Gas Chromatography (GC), Gas Chromatography-Mass Spectrometry (GC-MS), API gravimetry, elemental analysis, and isotope-ratio mass spectrometry (IR-MS) were carried out on eleven oil samples from the Sarvak reservoir in the Abadan Plain (SW Iran). Oil chemical composition, source, thermal maturity, age, lithology, and depositional environment of these oils' source rock were determined in this study. Moreover, Sarvak oils are mainly naphthenic and paraffinic type. Their API degree between 16.2 and 20.14 and about 4.6% sulfur content indicate heavy and sulfur-rich oils. The results of the study of biomarkers, stable carbon isotope composition, trace elements, aromatic and sulfur content indicated that all oil samples are related to a marine-carbonate source rock with strongly anoxic conditions. The absence of oleanane in all oil samples, the variation of Pr/Ph versus  $\delta^{13}\text{C}$  of the whole oil, and  $\text{C}_{28}/\text{C}_{29}$  steranes versus geological age proved that these oils had been produced earlier than the Late Cretaceous. Furthermore, the distribution of n-paraffins, calculation of Rc (%) from aromatic compounds, CPI (Carbon Preference Index) from gas chromatograms, and biomarker maturity indices indicated that the Sarvak oils are mature. Although the Sarvak oils are heavy, they show approximately maturity of peak oil-generative window, which represents a challenge in this study. It is guessed that the high sulfur content and low API gravity in the Sarvak reservoir oils are due to the presence of sulfur-rich organic matter (type IIS kerogen) in the source rock.

**Key words:** Crude oil inversion, Biomarkers, Sarvak reservoir, Abadan Plain, Southwest Iran.

### **Introduction**

Petroleum geochemistry is the practical application of organic geochemistry to the exploration and production of petroleum [1]. The Petroleum geochemical study of hydrocarbon reservoirs requires biomarker and non-biomarker parameters. The main purpose of the reservoir geochemistry is to identify the origin of oil, its maturity and biodegradation, heterogeneity of reservoir fluid, and reservoir connectivity. The other purpose of the reservoir geochemistry is to identify the compartments, which will lead to improved productivity, enhanced oil recovery, development of an oil field and reducing exploration risk [2,-4]. The crude oil inversion technique uses the crude oil's geochemical characteristics to provide clues about the nature of the source rocks that generated it [5]. Biomarkers are among the most effective means of studying crude oil inversion. The importance of biomarkers study has recently been well

recognized in the petroleum industry because it presents valuable information about the type of organic matter, environmental conditions during deposition (diagenesis), thermal maturity of crude oil or source rock, biological degradation, lithology of the source rock, and age of generated oils for geologists and petroleum engineers. Furthermore, combining biomarker and non-biomarker parameters can be used in better interpretation to resolve problems in exploration, development, and production [6]. The depositional environment and thermal maturity based on biomarker distributions have also been widely interpreted in 2005 by Peters et al [6]. The study of trace elements (especially nickel and vanadium) and stable carbon isotopes in crude oil inversion studies are widely applied and successfully used [7-10]. This study mainly focuses on the crude oil inversion technique to understand the source rock's characteristics that generated Sarvak oils in the studied oil field in the Abadan Plain,

\*Corresponding author: Ali Shekarifard, Oil and Gas Engineering Group, School of Chemical Engineering, College of Engineering, University of Tehran, Tehran, Iran

E-mail addresses: ashekary@ut.ac.ir

Received 2020-03-02, Received in revised form 2020-09-07, Accepted 2020-09-19, Available online 2020-11-22



southwest Iran.

### Geological Setting And Stratigraphy

The studied oilfield is located in the Abadan Plain (passive margin of Arabian Plate), as seen in Figure 1a. This area is located in the southwest of the Zagros fold-thrust belt, and it is surrounded by the Dezful Embayment, the Persian Gulf, and the Iran-Iraq boundary [11-13]. The Abadan Plain is a part of the Mesopotamian Basin, and its structural features are different from the Dezful Embayment [14].

Several studies have been undertaken on the potential source rocks in the Mesopotamian Basin and Abadan Plain [14-18]. The three main source rocks with extensive expansion in the Abadan Plain are Jurassic to Cretaceous units, which include Kazhdumi (Albian shale and marls), Garau (Lower Cretaceous carbonates), and Sargelu (Middle Jurassic carbonates) formations [15- 21].

The Cretaceous Sarvak Formation is one of the most important reservoirs in the Zagros Fold Belt in Iran's southwest [20]. The Sarvak Formation, as a member of the Bangestan group, is composed mainly of limestone with partially dolomitic layers. In the study area, the Sarvak Formation is located on the Kazhdumi Formation, and its upper contact is Laffan Shales (in Khuzestan), which is known as a cap rock for the Sarvak reservoir. In Figure 1b, a Cretaceous stratigraphic column of the Sarvak Formation in the studied area is shown [22]. This formation is applied to interpret deposition in a shallow-marine setting during the Cenomanian-Turonian. The depositional environment of this formation is a carbonate ramp [23]. This formation includes two main facies: (1) shallow marine (neritic) facies with limestones containing large foraminifera, gastropods, pelecypods, and rudist, (2) basinal (pelagic) facies or oligostegina facies rich in micritic and argillaceous limestone [24]. Moreover, the Sarvak Formation is affected by uplifting in the Late Cretaceous (Turonian), which resulted in extensive erosion and karstification. The karstification process increased the quality of this reservoir. In addition to karstification, the other processes, such as dolomitization, fracturing, dissolution, micritization, recrystallization, and cementation, affected the reservoir quality of the Sarvak Formation in the studied area

[25]. The oil intervals primarily include the Sar-8 in SEQ-4 and the Sar-3, 4, 5, 6 in SEQ-5. Sar-1 and Sar-2 zones are the dense regional interlayers of marl, mudstone, and shale, and the Sar-7 is mud/wackestone containing poor oil [19].

### Materials and Methods

#### Samples and Methods

Eleven liquid hydrocarbons from drill stem test (DST), repeat formation test (RFT), and also nineteen core plugs extract samples were obtained from six wells in one of the oil fields of SW Iran. All samples were from Sar-2, 3, 5, 6, 7 zones of the Sarvak reservoir with Cretaceous age.

In this study, the crude oil inversion technique was used. This technique is a modern approach that uses certain aspects of crude oil's geochemical properties to indicate some of the characteristics of its source rock, such as kerogen type, depositional setting, lithology, maturity, and, in some cases, the geologic age [1]. Based on this method, geochemical information obtained from crude oil, such as gas chromatographic data, stable carbon isotope composition ( $\delta^{13}\text{C}$ ), biomarkers, and metal elements (nickel and vanadium), has been used to interpret the conditions and type of depositional environment of source rock for the Sarvak reservoir oil samples.

The oil samples were analyzed using gas chromatography-flame ionization detector (GC-FID), gas chromatography-mass spectrometry (GC-MS), thin-layer chromatography-flame ionization detector (TLC-FID), and isotope-ratio mass spectrometry (IR-MS) instruments.

All core plugs were cleaned with water and dried at the laboratory temperature (25°C). The bitumen was extracted from core plugs by a 50 ml solvent containing a mixture of 90% dichloromethane (DCM) and 10% methanol (MeOH). First, asphaltenes from live oil and extracted bitumen were precipitated in the laboratory using normal hexane followed by filtration. Then using column chromatography, the deasphalted oil was fractionated to saturate, aromatic, and polar (NSO) by eluting with n-hexane, benzene and methanol, respectively.

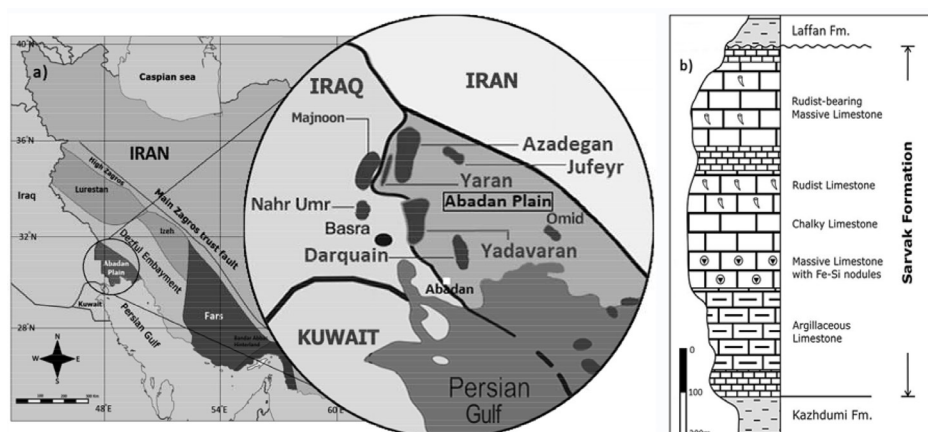


**Fig. 1** a) Map of Zagros structural divisions and geographical location of the studied area (Abadan Plain), b) The sedimentary sequence of the Sarvak Formation [22].

The whole oil was separated into saturated, aromatic, and polar compounds (resins + asphaltenes) by Iatroscan MK-5 thin-layer chromatography-flame ionization detection (TLC-FID) instrument equipped with a flame ionization detector (FID).

Gas chromatography analysis carried out using a Hewlett-Packard 5890 gas chromatograph equipped with a 30 m x 0.25 mm capillary column bearing 0.25  $\mu\text{m}$  film thickness and a flame ionization detector (FID). The oven temperature was programmed for 40 to 300  $^{\circ}\text{C}$  at 5  $^{\circ}\text{C}/\text{min}$ , with a final holding temperature at 300  $^{\circ}\text{C}$  for 30 min.

Gas chromatography-mass spectrometry (GCMS) of saturated and aromatic fractions was carried out on a Micromass ProSpec instrument equipped with a 60 m x 0.25 mm capillary column bearing 0.25  $\mu\text{m}$  film thickness. The column oven was programmed from 50 to 350  $^{\circ}\text{C}$  at 2  $^{\circ}\text{C}/\text{min}$ , and then it was held for 30 min at 300  $^{\circ}\text{C}$ . The saturated and aromatic hydrocarbon biomarkers were calculated from peak heights on the mass chromatograms.

To obtain stable carbon isotope ratios in this study, a Horizon 2-IRMS instrument which is connected to the gas chromatography apparatus described above, was used by us. In this analysis, the gas column and temperature program used were similar to those in GC-MS analysis.

Helium (He) was selected as the carrier gas in all of the instruments in this study.

## Results and Discussion

### Characteristics of Bulk Oil

In this study, the bulk oil is divided into four fractions: saturate and aromatic (hydrocarbons), resin, and asphaltene (NSO

components). The percentage of oil components obtained from Iatroscan analysis (TLC-FID) for several wells in the studied field is shown in Table 1. As shown, the oils have relatively high polar compounds (resin and asphaltene) and relatively low saturating fraction values, except well B, which has a high saturate fraction (maturity parameters indicate that the oil samples from this well have the highest maturation). The Tissot and Welte ternary diagram (1984) have also been used to determine the type of oil group (family), as seen in Figure 2 [26]. This diagram illustrates that samples of oil from the Sarvak reservoirs are mostly naphthenic and paraffinic.

According to Table 2, the oil samples of the Sarvak reservoir in the studied field have an API degree between 16.2 and 20.14. On the other hand, the sulfur content of samples has an average of 4.6%, which is relatively high. Therefore, high values of polar compounds and sulfur content and low API indicate heavy oils. A low API degree and a high percentage of sulfur in crude oil can represent biodegradation or low maturation [27]. However, the oil samples of the Sarvak reservoir in this field have not been probably affected by biodegradation (due to the presence of n-alkanes in the  $\text{C}_6$  to  $\text{C}_{12}$  range, the absence of unresolved complex mixture-UCM, and also, low  $\text{Pr}/\text{nC}_{17}$  and  $\text{Ph}/\text{nC}_{18}$  ratios in the gas chromatograms of the Sarvak reservoir oil samples in this study [6]). The maturity parameter indices (such as biomarkers or aromatic compounds) represent the maturity of peak oil generation for the Sarvak reservoir oils in this study. Therefore, high sulfur content and low API degrees of oils probably indicate that those are generated from marine-carbonate source rock under anoxic conditions and contain type II-S kerogen [28].

**Table 1** Results of Iatroscan TLC-FID analysis for the oil samples of the Sarvak reservoir. Polar: Resin + Asphaltene (all of the values in this table are the average of several oil samples from each well).

Well	Saturate (%)	Aromatic (%)	Resin (%)	Asphaltene (%)	Polar(%)
A	36.86	18.57	36.29	8.27	44.56
B	60.27	4.41	28.06	7.26	35.32
D	42.71	6.04	47.42	3.82	51.24
E	28.62	10.95	54.12	6.31	60.43

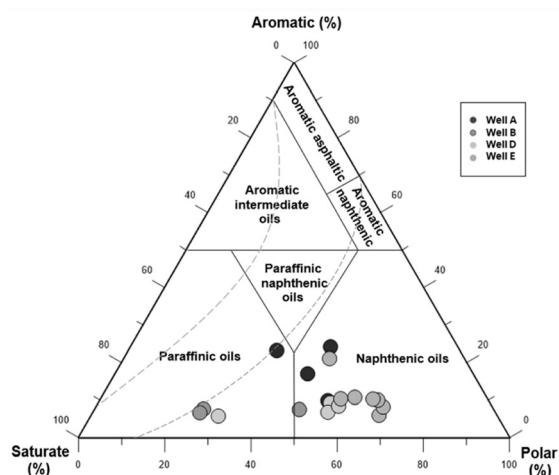


**Fig. 2** Ternary diagram of various crude oil components which is used to represent the type of oil family related to the oil samples of the Sarvak reservoirs. The samples are mainly in the naphthenic and paraffinic zones (diagram from [26]).

**Table 2** Bulk property and chemical composition of the crude oils from the Sarvak reservoir in one of the oil fields of southwest Iran. S, Ni, and V stand for Sulfur, Nickel, and Vanadium, respectively.

Well	Samples ID	Interval (m)	API gravity	S(Wt.%)	Ni(ppm)	V (ppm)	V/Ni	V/(V+ Ni)
B	S01	2762-2778	19.94	0.27	48	124	2.5	0.72
B	S03	2762-2778	-	-	-	-	-	-
B	S04	2800-2820	18.10	-	-	-	-	-
C	S02	2928-2938	16.20	5.1	37	182	4.9	0.84
C	S05	2928-2938	-	-	-	-	-	-
C	S06	2806-2821	17.30	4.6	36	112	3.1	0.75
C	S07	2806-2821	-	-	-	-	-	-
D	S08	2654-2664	18.50	5	38.01	107.28	2.8	0.73
D	S09	2765-2778	20.14	3.24	25	81	3.24	0.76
E	S18	3024-3035	19.50	-	-	-	-	-
F	S21	2692-2725	19.50	5.44	29.1	98.82	3.3	0.77
Well	Samples ID	Interval (m)	API gravity	S(Wt.%)	Ni(ppm)	V (ppm)	V/Ni	V/(V+ Ni)
B	S01	2762-2778	19.94	0.27	48	124	2.5	0.72
B	S03	2762-2778	-	-	-	-	-	-
B	S04	2800-2820	18.10	-	-	-	-	-
C	S02	2928-2938	16.20	5.1	37	182	4.9	0.84
C	S05	2928-2938	-	-	-	-	-	-
C	S06	2806-2821	17.30	4.6	36	112	3.1	0.75
C	S07	2806-2821	-	-	-	-	-	-
D	S08	2654-2664	18.50	5	38.01	107.28	2.8	0.73
D	S09	2765-2778	20.14	3.24	25	81	3.24	0.76
E	S18	3024-3035	19.50	-	-	-	-	-
F	S21	2692-2725	19.50	5.44	29.1	98.82	3.3	0.77

## Gas chromatography (GC)

### Normal Alkanes

In this study, eleven representative oil samples were selected for the gas chromatographic analysis. All of the identifiable peaks were numbered from C<sub>5</sub> to C<sub>25</sub> carbon number range, as seen in Figure 3. Similar general patterns were observed with the bell-shaped and mainly unimodal distribution of normal alkanes in all gas chromatograms of the oil samples. More abundance of normal alkanes is approximately in the range of light to medium hydrocarbons.

A slight even/odd n-alkane predominance is recognizable in the gas chromatograms of the oil samples.

The oil samples may exhibit a different distribution of n-alkanes by gas chromatography because they may have been generated from several sources or are affected by secondary processes. Therefore, studying oils for assessment of reservoir geochemistry (especially oil-oil correlation) using the only distribution of normal alkanes would be wrong [6].

Distribution and abundance of normal paraffin can be used to determine the maturation (section 5.1) and the origin of oils. These interpretations are performed by studying the peaks of the gas chromatograms of the whole oil. The oils generated from the organic amorphous and sapropelic materials are characterized by the highest frequency of C<sub>15</sub>-C<sub>25</sub> peaks indicating the origin of marine oil [6]. On the other hand, the oil generated from terrigenous organic matter (vascular plants) has the highest frequency in normal paraffin of C<sub>25</sub>-C<sub>29</sub> in the gas chromatograms [29].

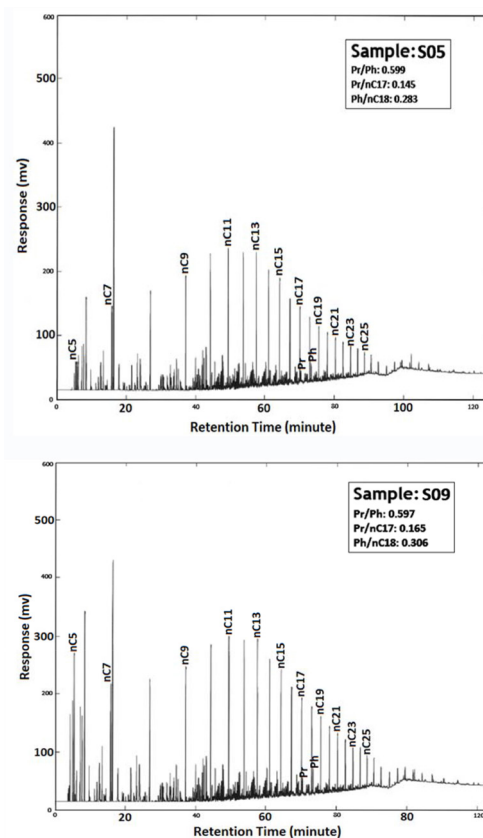


**Fig. 3** Two representative gas chromatograms of whole oil (sample S05 and S09 from well C and D, respectively) related to the Sarvak reservoir in the studied field (Pr: Pristane, Ph: Phytane).

Also, the bimodal distribution of n-paraffins in gas chromatograms is mainly related to waxy terrigenous oils. However, the unimodal distribution of n-paraffins shows the oils which are generated from marine source rocks. It should be noted that often immature oils can also show bimodal properties [1,6].

As shown in Figure 3, all gas chromatograms of the Sarvak reservoir oils have a certain range of light to moderate ( $C_5$  to  $C_{25}$ ) n-alkanes. Due to the very low presence of heavy n-alkanes ( $nC_{25}<$ ) in gas chromatograms and the more abundance of n-alkanes with less than 25 carbon numbers ( $nC_{25}>$ ), as well as almost the lack of bimodal distribution of n-alkanes, it can be stated that the all the Sarvak reservoir oils are essentially originated from marine organic matters.

TAR or terrigenous/aquatic ratio is one of the best parameters for recognition of terrigenous versus aquatic organic matter input from some peaks of n-alkanes by gas chromatograms. This parameter is calculated from Equation 1:

$$TAR = (nC_{27} + nC_{29} + nC_{31}) / (nC_{15} + nC_{17} + nC_{19}) \quad (1)$$

The calculated TAR in this study indicates very low values (average: 0.14 in Table 3) and proves that the Sarvak reservoir oils in the studied field are essentially from marine sources [30].

**Table 3** Parameters calculated from GC-FID chromatograms of the crude oils from the Sarvak reservoir, CPI: Carbon preference index. TAR: Terrigenous aquatic ratio.

Well	Samples ID	CPI	TAR
B	S01	0.98	0.14
B	S03	0.96	0.15
B	S04	0.97	0.28
C	S02	1.03	0.14
C	S05	0.97	0.15
C	S06	0.95	0.07
C	S07	0.98	0.06
D	S08	1.01	0.15
D	S09	0.98	0.14
E	S18	0.97	0.15
F	S21	1	0.15

#### Acyclic Isoprenoids (Saturated Biomarkers)

This group of biomarkers has a linear structure built up of Isoprene units. Two important types of acyclic isoprenoids, which are very useful in detecting source rock conditions, are pristane and phytane [28].

An increase in pristane relative to phytane indicates that the source rock is deposited in an oxic environment (such as the peat bogs) and vice versa. The phytane increase relative to pristane represents a source rock with an oxic depositional environment [28,31]. Peters et al. suggested that the high ratio of pristane to phytane (more than 3) indicates the continental (terrigenous) organic matter input and the source rock with oxic conditions, while low values of this ratio (less than 0.8) represent the marine carbonate depositional environment and an oxic conditions [6]. As shown in Figure 3, all gas chromatograms of the analyzed Sarvak reservoir oils display low pristane values relative to phytane (Pr/Ph:

0.566 to 0.908 in Table 4). Therefore, the slight even/odd n-alkane predominance and the low Pr/Ph values suggest likely the abundance of algal organic matter and type II-S kerogen deposited under reducing conditions.

A useful plot of the  $Ph/nC_{18}$  against  $Pr/nC_{17}$  was presented by Talukdar et al. in 1993 and Hunt in 1996 [28,32]. In this plot, valuable information about the source rock, including its reduction or oxidation, type of kerogen, the relative levels of maturity, and biodegradation of the oil can be obtained. This plot has been used for the Sarvak reservoir oils (Figure 4). In this figure, the oil samples are all located in the range of marine source rock under reducing conditions, and they are rich in type II kerogen.

#### Terpenes

In this study, terpenes were monitored using m/z 191 mass chromatogram by GC-MS instrument. Hopanes, as one of the types of terpenes, are a subset of triterpenes with five carbon rings, and they are found in the cell membrane of prokaryote organisms such as bacteria. Therefore, the abundance of these biomarkers in crude oil shows that the amounts of bacterial source input have been high [6,28]. The most important hopanes in crude oils include Bisnorhopane, Trisnorhopane, Gammacerane, and Oleanane.

$C_{35}/C_{34}$  hopane ratios for Sarvak reservoir oil samples are values ranging from 1.440 to 1.211 (average: 1.304). The high values of  $C_{35}/C_{34}$  hopanes (greater than 1) indicate strongly reducing conditions [6]. Also, it was found out by Connan et al. in 1986 that  $C_{29}/C_{30}$  hopane ratios for carbonate environments are more than 0.8 [33]. The Sarvak oils have  $C_{29}/C_{30}$  hopane ratios from 1.125 to 1.208 (average: 1.164). Therefore, high values of  $C_5/C_{34}$  and  $C_{29}/C_{30}$  hopane ratios in the oil samples represent a source rock that is deposited in a carbonate environment under strongly anoxic conditions. To better understand the above description, a cross-plot of  $C_{29}/C_{30}$  hopanes versus  $C_{35}/C_{34}$  hopanes has been drawn, as seen in Figure 5.

One of the important parameters for evaluating oil and source rock maturity is  $Ts/(Ts+Tm)$  Trisnorhopane ratio [28]. The full names of Ts and Tm are trisnorhopane-18 $\alpha$ (H)-22,29,30 and trisnorhopane-17 $\alpha$ (H)-22,29,30, respectively.  $Ts/(Ts+Tm)$  appears to be sensitive to clay-catalyzed reactions. For example, oils from carbonate source rocks have low  $Ts/(Ts+Tm)$  ratios compared to those from shales [33]. The  $Ts/(Ts+Tm)$  in this study is between 0.146 to 0.173 (average: 0.16). Since the Sarvak reservoir oils in this field have a marine-carbonate source rock, the low  $Ts/(Ts+Tm)$  ratios in this study could be due to marine-carbonate minerals and the absence of clay-catalyzed reactions in the source rock. However, increasing thermal maturity can also reduce this ratio. Oleanane index (oleanane/oleanane +  $C_{30}$  hopane) as one of the most suitable source indicators is used for identifying the origin of the oils with deltaic sedimentary environments and the amounts of organic matter inputs of terrestrial plants to the environment, especially the Angiosperms, which are associated with Upper and younger Cretaceous. The oleananes are probably derived from the five-ring triterpenes secreted from angiosperms [35].

According to Table 4, the oleanane index for all samples is equal to 0.00.

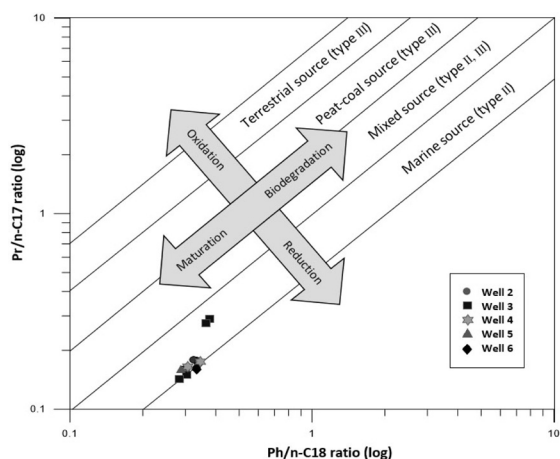


**Fig. 4** Plot of Ph/n-C<sub>18</sub> against Pr/n-C<sub>17</sub> for the Sarvak reservoir oils in the studied field. As can be seen, the oil samples have been generated from a marine-carbonate source rock and probably rich in type II kerogen [28,32].

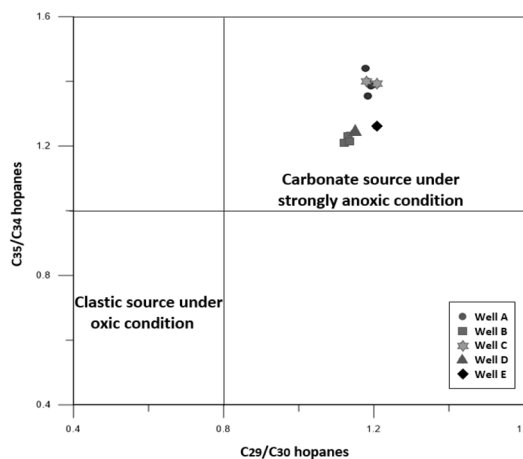


**Fig. 5** Cross-plot of C<sub>29</sub>/C<sub>30</sub> hopanes against C<sub>35</sub>/C<sub>34</sub> hopanes for Sarvak oil samples in the studied field. In this plot, all samples belong to a carbonate source rock with strongly anoxic conditions.

**Table 4** GC-MS data as calculated from mass chromatogram peaks of the crude oils from the Sarvak reservoir in the studied area (Isoprenoids, Terpenes, and Steranes).

Well	Samples ID	Isoprenoids			Steranes (m/z 217)					Terpenes (m/z 191)							Hopane/Sterane	
		pri/ph	pri/nC <sub>17</sub>	ph/nC <sub>18</sub>	C <sub>27</sub> (%)	C <sub>28</sub> (%)	C <sub>29</sub> (%)	C <sub>28</sub> /C <sub>29</sub>	dia/st+dia	20S/20S+R ααα C <sub>29</sub> sterane	ββ/ αα+ββ C <sub>29</sub> sterane	Ts/ Ts+Tm	C <sub>29</sub> / C <sub>30</sub>	C <sub>35</sub> / C <sub>34</sub>	C <sub>32</sub> / 22S/22S+R homohopane	G/C <sub>30</sub>		Ol/ C <sub>30</sub>
B	S01	0.59	0.178	0.332	0.312	0.274	0.414	0.66	0.093	0.556	0.637	0.173	1.177	1.44	0.581	0.013	0	0.91
B	S03	0.566	0.171	0.339	0.309	0.27	0.421	0.641	0.096	0.537	0.642	0.172	1.184	1.355	0.577	0.013	0	0.89
B	S04	0.618	0.179	0.324	0.297	0.271	0.431	0.629	0.094	0.523	0.641	0.17	1.192	1.386	0.578	0.013	0	0.91
C	S02	0.623	0.157	0.3	0.319	0.264	0.417	0.635	0.074	0.536	0.633	0.146	1.133	1.234	0.573	0.013	0	0.85
C	S05	0.599	0.145	0.283	0.301	0.24	0.459	0.522	0.075	0.53	0.624	0.147	1.131	1.214	0.575	0.013	0	0.87
C	S06	0.908	0.287	0.372	0.297	0.258	0.445	0.581	0.095	0.489	0.613	0.148	1.125	1.213	0.574	0.012	0	0.86
C	S07	0.89	0.278	0.367	0.321	0.245	0.433	0.566	0.092	0.501	0.625	0.149	1.127	1.211	0.574	0.012	0	0.86
D	S08	0.591	0.176	0.342	0.324	0.252	0.424	0.594	0.094	0.533	0.64	0.17	1.208	1.39	0.577	0.013	0	0.92
D	S09	0.597	0.165	0.306	0.316	0.261	0.423	0.616	0.079	0.53	0.637	0.162	1.181	1.4	0.578	0.013	0	0.91
E	S18	0.63	0.16	0.294	0.314	0.247	0.438	0.564	0.069	0.546	0.639	0.16	1.148	1.243	0.572	0.012	0	0.87
F	S21	0.572	0.162	0.333	0.278	0.274	0.448	0.612	0.082	0.553	0.64	0.167	1.206	1.262	0.577	0.01	0	0.88

Pr: Pristane. Ph: Phytane.

C<sub>27</sub> (%): C<sub>27</sub>/C<sub>27</sub>+C<sub>28</sub>+C<sub>29</sub> regular sterane.

G/C<sub>30</sub>: Gammacerane/C30 hopane

Tm: C<sub>27</sub> 17a(H)-22,29,30-trisnorhopane.

C<sub>35</sub>/C<sub>34</sub>: C<sub>35</sub>/C<sub>34</sub> hopane.

Ts: C<sub>27</sub> 18a(H)-22,29,30-trisnorhopane.

C<sub>29</sub>/C<sub>30</sub>: C<sub>29</sub>/C<sub>30</sub> hopane.

C<sub>28</sub> (%): C<sub>28</sub>/C<sub>27</sub>+C<sub>28</sub>+C<sub>29</sub> regular sterane

Ol/C<sub>30</sub>: Oleanane/Oleanane + C<sub>30</sub> hopane

C<sub>29</sub> (%): C<sub>29</sub>/C<sub>27</sub>+C<sub>28</sub>+C<sub>29</sub> regular sterane.

Therefore, due to the absence of oleanane in all samples of the Sarvak reservoir in this field, it can be said that the oils of this reservoir are derived from a source rock older than the Upper Cretaceous and Tertiary, which the source rock does not have terrigenous plants organic matter input, such as angiosperms (flowering plants) and younger than the angiosperms. However, it should be noted that the absence of oleanane does not always prove that crude oil is generated from Cretaceous or older rocks [6].

Gammacerane indicates a stratified water column in marine and non-marine source rock depositional environments resulting from hypersalinity at depth [36]. An increase in salinity of the depositional environment results in a high concentration of gammacerane. Among biomarker data, as seen in Table 4, gammacerane index (gammacerane/gammacerane+C30hopane) is very slight (average: 0.01). It may indicate the low salinity of the source rock depositional environment of the Sarvak reservoir oils.

### Steranes and Diasteranes

Steranes and diasteranes are displayed in the m/z 217 mass chromatograms. C<sub>27</sub>, C<sub>28</sub>, and C<sub>29</sub> steranes are most commonly found in algae, marine organisms, and higher plants, respectively [37]. These biochemical molecules are derived from eukaryotic organisms [38]. The restructuring of the steranes also causes diasteranes.

Using ternary diagrams of the C<sub>27</sub>, C<sub>28</sub>, and C<sub>29</sub> regular steranes, the source rock's characteristics can be determined based on the type of organisms generating oil and sedimentary environment [28,37,39,40]. In Figure 6 (a, b and c), an example of ternary diagrams of C<sub>27</sub>, C<sub>28</sub>, and C<sub>29</sub> regular steranes for oil samples from the Sarvak reservoir is shown. In these three diagrams, all oil samples from this reservoir are limited to the marine-carbonate environment, and they are rich in planktonic organic matter.

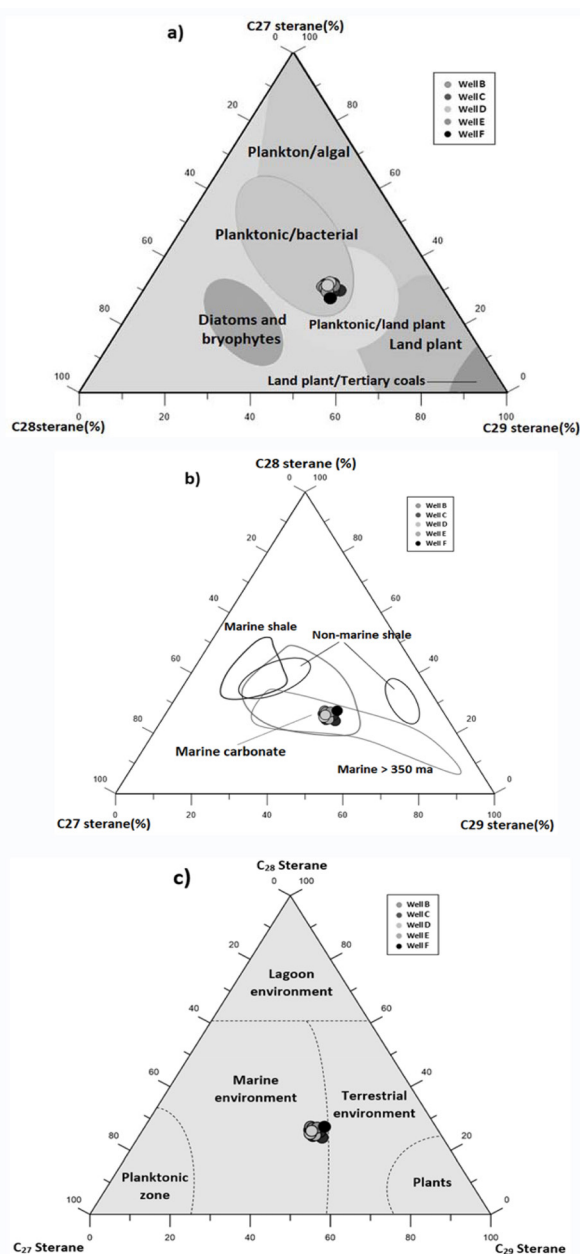


**Fig. 6** Determination of relationships between sterane homologs ( $C_{27}$ ,  $C_{28}$ , and  $C_{29}$ ) for the study of organic matter input and depositional environment of source rock for the Sarvak reservoir oil samples in the studied oil field. a: Ternary diagram of  $C_{27}$ ,  $C_{28}$ , and  $C_{29}$  regular steranes show the type of oil-generating microorganisms [37] and b, c: Ternary diagrams of  $C_{27}$ ,  $C_{28}$ , and  $C_{29}$  regular steranes show the type of depositional environment of the source rock (both diagrams indicate marine depositional environment for the source rock of Sarvak oils) [37, 40].

As shown in Table 4, the abundance of  $C_{29}$  regular steranes is higher than that of  $C_{27}$  and  $C_{28}$  regular steranes. Although more abundance of  $C_{29}$  regular steranes in crude oils indicate a strong land plant terrestrial contribution, the abundance of  $C_{29}$  regular steranes in this study cannot express the origin of oil from land plants. Because, according to the previous studies, [41-43], the abundance of  $C_{29}$  regular steranes in marine and pelagic carbonate source is mainly due to  $C_{29}$  sterols secreted from the microalgae (e.g. diatoms). By considering all oil samples in this study, it is found out that the source is marine-carbonate; also, all oil samples have low TAR values (Table 3); therefore, these oils are probably

related to deep-marine microorganisms.

There is a general increase in the relative content of  $C_{28}$  steranes, and also, there is a decrease in  $C_{29}$  steranes in marine petroleum through geologic time [6,40,44].  $C_{28}/C_{29}$  steranes are less than 0.5 for Lower Paleozoic and older oils, 0.4 – 0.7 for Upper Paleozoic to Lower Jurassic oils, and greater than ~0.7 for Upper Jurassic to Miocene oils [44]. Average value of  $C_{28}/C_{29}$  sterane ratio for Sarvak oil samples is 0.601 (minimum= 0.52 to maximum= 0.66) (Table 4). This value indicates that the oils are related to Upper Paleozoic to Triassic and Lower Jurassic. Figure 7 shows that the variation of the  $C_{28}/C_{29}$  sterane ratio versus geological time, together with the oil-producing microorganisms for the Sarvak reservoir oils, is illustrated. As can be seen, the  $C_{28}/C_{29}$  ratio covers the range of dinoflagellates and coccolithophorids (Shaded area). Also, this range intersects a hypothetical curve in Jurassic, Triassic, and Permian. It corresponds to the absence of an oleanane biomarker in the Sarvak oil samples.

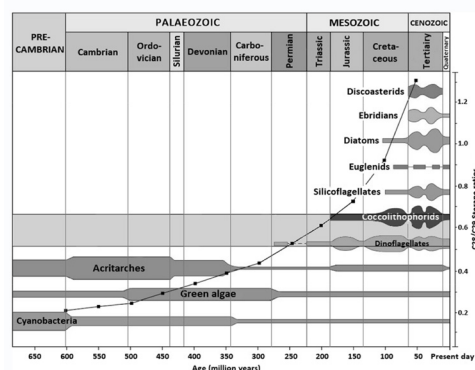


**Fig. 7** Relationship between the geological age and  $C_{28}/C_{29}$  steranes for oils from marine organic matter source [44]. The shaded area is related to  $C_{28}/C_{29}$  sterane ratios for Sarvak reservoir oils.

Carbonate source rocks tend to have lower amounts of diasteranes [6]. As a result, low values of diasteranes/diasteranes + sterane ratios sometimes indicate carbonate environments. Moreover, diasteranes/diasteranes + sterane ratios in oil samples from the Sarvak reservoir range from 0.069 to 0.096, with an average of 0.085 that represents very low values (Table 4), indicating marine-carbonate source rock for the studied oils.

Therefore, it seems that the very low values of diasterane/diasterane + sterane and  $T_s/T_s+T_m$  ratios in this study have not been affected by the maturation of oil.

#### Elemental Analysis (Trace Elements)

Nickel and vanadium are inherited from the source rocks in Porphyrin molecules. Therefore, the final crude oil contains information about the source rock's Ni/V ratio [1]. The crude oils from the marine carbonate source rock include a low Ni/V ratio, low wax, and high sulfur content. Vanadium, more than a nickel in such environments, can be due to reducing conditions of source rock, which this state of vanadium in the structure of porphyrin is more stable than a nickel. The oils generated from terrigenous organic matter (lacustrine) have high wax, low sulfur content, and high Ni/V ratios [28]. In Figure 8, the  $V/(V+Ni)$  against sulfur content (wt.%) for oil samples from the Sarvak reservoir is demonstrated. The oil samples in this plot belong to the marine carbonate source rock deposited under anoxic conditions [45].

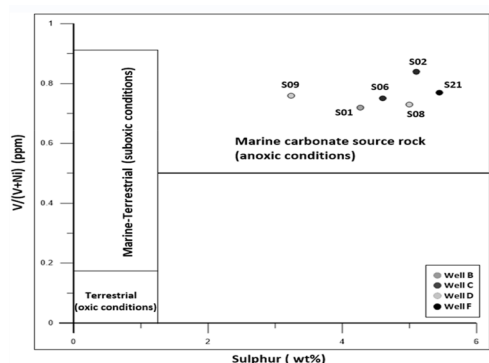


**Fig. 8** Cross-plot of sulfur content (%) versus V/(V + Ni) of the analyzed samples in ppm for Sarvak reservoir oils in the studied field. The samples are related to a marine carbonate source rock that was deposited under anoxic conditions [45].

Changing the vanadium to nickel ratios is also possible to determine the type of depositional environment and oxic or anoxic conditions of source rock. It means that the ratios of V/Ni more than 3 represent anoxic conditions. V/Ni ratios between 1.9 and 3 represent sub-oxic conditions, and V/Ni less than 1.9 account for the completely oxic environments [46]. The V/Ni ratios of analyzed oil samples from the Sarvak reservoir range from 2.5 to 4.9 (average: 3.3 in Table 2), indicating that the source rock of these oils deposited in a sedimentary environment under mainly reducing conditions.

**Stable Carbon Isotope Composition ( $\delta^{13}C$ )**

One of the most important means in the study of crude oil inversion is the carbon isotope ratio ( $\delta^{13}C$ ) of oil samples [7]. By calculating a parameter called “Canonical Variable” (CV) and plotting it against Pristane/Phytane ratio, the source rock conditions for oil samples can be determined. The values of CV can be calculated from Equation 2 [47]:

$$CV = -2.53 \sigma^{13}C_{saturate} + 2.22 \sigma^{13}C_{aromatic} - 11.65 \quad (2)$$

CV for waxy terrigenous oils is more than 0.47 (CV > 0.47). This value is less than 0.47 (CV < 0.47) for marine and non-waxy oils [47]. In Table 5, stable carbon isotope composition and calculated CV for the Sarvak reservoir oils are shown. In Figure 9, CV values have been plotted against the Pristane/Phytane ratio. This plot indicates that the oil samples are completely related to the marine source rock with anoxic (reducing) conditions.

Using the graph of carbon isotope ratio ( $\delta^{13}C$ ) of whole oil against Pristane/Phytane ratios can also be determined the age and depositional environment of source rock [48]. Figure 10a illustrates this graph for oil data from the Sarvak reservoir in the studied field. All samples are located in the Mesozoic carbonate source rock range.

**Table 5** Stable carbon isotope ratios ( $\delta^{13}C$ ) and CV values for three representative Sarvak reservoir oil samples.

Well	SamplesID	$\delta^{13}C$ (‰)Sat	$\delta^{13}C$ (‰)Aro	$\delta^{13}C$ (‰) Whole oil	CV
C	S02	-27.23	-27.78	-27.39	-4.43
C	S06	-27.35	-27.75	-27.33	-4.06
D	S08	-27.47	-27.72	-27.48	-3.69

Sat stands for Saturate, Aro stands for Aromatic, and CV stands for Canonical variable.

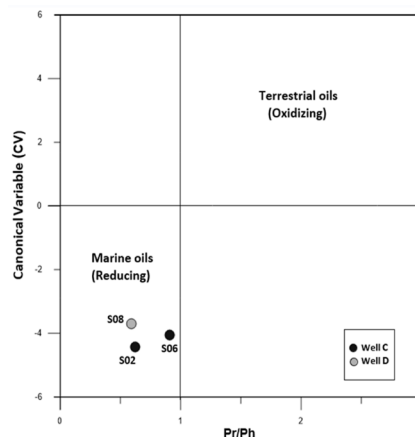


**Fig. 9** Cross-plot of calculated CV values versus Pr/Ph ratios for Sarvak reservoir oil samples. As can be seen, these oils have a marine source rock with reducing conditions [47].

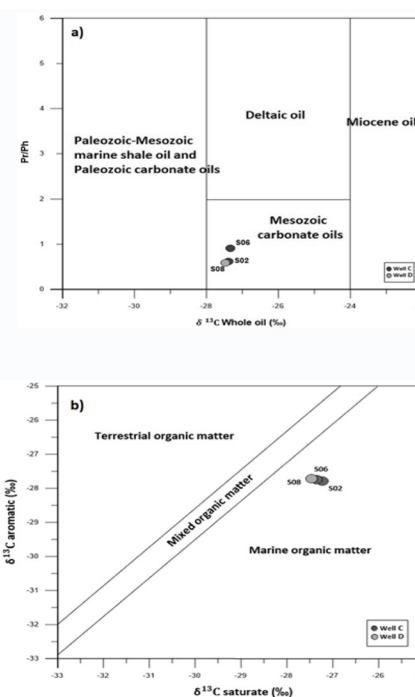


**Fig. 10:** a) Cross-plot of Pr/Ph ratio versus  $\delta^{13}C$  of whole oil that shows a marine-carbonate environment for the source of Sarvak reservoir oils in the studied field [48]. b) Stable carbon isotope ratios (in per mille) for saturated versus aromatic hydrocarbons. This plot demonstrates that the source rock for Sarvak reservoir oils is derived from mainly marine organic matter (modified after [47]).

The carbon isotope ratio of saturated and aromatic oil fractions has well introduced its efficiency for studying source rocks. Sofer (1984) determined Two types of sedimentary environment for source rocks by plotting the carbon isotope ratio of these two hydrocarbon fractions against each other in 1984 [47]. This plot is used for the Sarvak reservoir oils (Figure 10b). In this plot, oil samples are located in the marine source rock area.

**Thermal Maturity**

**Maturity From Normal Alkanes And Isoprenoids**

Distribution of n-paraffins in over mature oils in the gas chromatograms is mostly unimodal. In this case, the distribution of n-alkanes moves toward the lighter part

of the oil, and it becomes unimodal [1]. In most cases, such as oils with low maturity, waxy terrigenous oils also have a bimodal gas chromatogram. In order to differentiate them, other parameters, such as biomarkers, are used [1,6]. In the gas chromatograms of Figure 3, the peaks related to heavy n-alkanes are very low. Therefore, the more abundance of hydrocarbons in these two gas chromatograms is related to light to medium n-alkane peaks ( $C_5$  to  $C_{25}$ ), representing mature oils.

As can be seen in the gas chromatograms of Figure 3, a slight abundance of n-alkanes with an even number of carbons relative to those with an odd number of carbons is mainly predominant. By increasing maturity, the abundance of n-alkanes with an even number of carbons will increase. However, the oils with lower maturation have an odd number of carbons predominance in n-alkanes [49].

Bray and Evans (1961) obtained a carbon preference index (CPI) for the range of  $C_{25}$  to  $C_{33}$  by studying the present sediments and crude oils [50]. It is calculated from Equation (3):

$$CPI = 0.5 \left[ \frac{\sum_{C_{21} \text{ to } C_{31}} \text{Odd } n\text{-Paraffins}}{\sum_{C_{22} \text{ to } C_{32}} \text{Even } n\text{-Paraffins}} + \frac{\sum_{C_{21} \text{ to } C_{31}} \text{Odd } n\text{-Paraffins}}{\sum_{C_{20} \text{ to } C_{30}} \text{Even } n\text{-Paraffins}} \right]$$

Oils with lower maturation or immature source rocks have a CPI more than 1, and oils with over maturation or mature source rocks have a CPI about 1 [49].

As shown in Table 3, the calculated CPI for oil samples is about 1. It indicates that the maturation of Sarvak reservoir oils is relatively high.

#### Aromatic Hydrocarbon Maturity Parameters

Methylphenantrene index (MPI-1) derived from thermal extract GC-MS for the Sarvak reservoir core samples is 0.71

to 0.82, indicating a high maturation level.

Vitrinite reflectance (%Rc) was calculated from MPI-1 and MDR (as seen in Table 6) according to Equations 4 and 5 [51]:

$$\%Rc = 0.6 \text{ MPI} - 1 + 0.4$$

$$\text{Where } \text{MPI} - 1 = 1.5 (3 - MP + 2 - MP) / (P + 9 - MP + 1 - MP).$$

(4)

$$\%Rc = 0.6 \text{ MPI} - 1 + 0.4$$

$$\text{Where } \text{MPI} - 1 = 1.5 (3 - MP + 2 - MP) / (P + 9 - MP + 1 - MP).$$

(5)

The calculated vitrinite reflectance (%Rc) based on MPI-1 values for the studied samples is in the range of 0.86 to 0.89 (average: 0.86), and the %Rc based on MDR is in the range of 0.64 to 0.69 (average: 0.66), indicating a high level of thermal maturation (approximately peak oil window).

All extracts of core samples in this study have MDR (4-MDBT/1-MDBT) between 1.9 and 2.47 (Table 6), indicating relatively high sulfur contents. High values of MDR correspond with a marine-carbonate source under strongly anoxic conditions. However, biodegradation may also have resulted in sulfur enrichment, as benzothiophenes and high molecular weight hetero-compounds are resistant to bacterial degradation [26]. In Figure 11, a cross-plot of MDBT/MP against Pristane/Phytane for the Sarvak reservoir oils in this field is shown. As shown, all samples related to marine-carbonate depositions, and they were rich in sulfur. Lower values of pristane relative to phytane additional high values of MDBT in this study (Table 4 and 6) prove the presence of  $H_2S$  gas caused by sulfate-reducing bacteria and rich sulfur organic matter (modified from [52]), [53].

**Table 6** Aromatic compounds and parameters calculated from GC-MS chromatograms for the Sarvak reservoir oils.

Well	MPI-1(m/z 192)	(MDR)(m/z 198)	MDBT/MP	%Rc (based on MPI-1)	%Rc (based on MDR)
A	0.800	2.472	3.09	0.88	0.69
B	0.774	2.081	2.68	0.86	0.66
D	0.714	1.903	2.66	0.82	0.64
E	0.826	2.414	2.92	0.89	0.68
Well	MPI-1(m/z 192)	(MDR)(m/z 198)	MDBT/MP	%Rc (based on MPI-1)	%Rc (based on MDR)
A	0.800	2.472	3.09	0.88	0.69
B	0.774	2.081	2.68	0.86	0.66
D	0.714	1.903	2.66	0.82	0.64
E	0.826	2.414	2.92	0.89	0.68
Well	MPI-1(m/z 192)	(MDR)(m/z 198)	MDBT/MP	(Rc (based on MPI-1%)	(Rc (based on MDR%)
A	0.800	2.472	3.09	0.88	0.69
B	0.774	2.081	2.68	0.86	0.66
D	0.714	1.903	2.66	0.82	0.64
E	0.826	2.414	2.92	0.89	0.68
Well	MPI-1(m/z 192)	(MDR)(m/z 198)	MDBT/MP	(Rc (based on MPI-1%)	%Rc (based on MDR)
A	0.800	2.472	3.09	0.88	0.69
B	0.774	2.081	2.68	0.86	0.66
D	0.714	1.903	2.66	0.82	0.64
E	0.826	2.414	2.92	0.89	0.68

$(PM-1 + PM-9 + P) / (PM-2 + PM-3) \times 5.1 = (\text{xedni enertnanehplyhtem})$  1-IPM .enertnanehplyhtem :PM  
enehpoihtoznebid lyhtem :TBDM

TBDM-1 /TBDM-4 = (oitar enehpoihtoznebid lyhtem) RDM

$4.0 + 1\text{-IPM} \times 6.0 = (1\text{-IPM no desab})$  cR%

$15.0 + RDM \times 370.0 = (RDM no desab)$  cR%

### Saturated Hydrocarbon Maturity Parameters

To evaluate thermal maturity of the Sarvak reservoir oils, some parameters based on saturated hydrocarbons, for example,  $C_{29}$  sterane  $\beta\beta/(\beta\beta+\alpha\alpha)$ ,  $C_{29}$  sterane 20S/20S+20R, Ts/Ts+Tm trisnorhopane,  $C_{32}$  22S/(22S+22R) homohopanes have been used [54,55]. The stability of  $\beta\beta$  configuration relative to  $\alpha\alpha$  and 20S configuration relative to 20R in  $C_{29}$  steranes becomes higher during thermal maturation. Therefore, by increasing thermal maturity, the ratio of  $\beta\beta/(\beta\beta+\alpha\alpha)$  and 20S/20S+20R will increase [6]. Homohopanes ( $C_{31}$ - $C_{35}$ ) occur in the 17 $\beta$ (H) configuration in immature sediments with only the 22R epimer. During the diagenesis stages, this epimer is gradually converted to a mixture of 22S and R with increasing maturity [28]. As a result, with an increase in crude oils' thermal maturity, the ratio of 22S/(22S+22R) also increases. Also, 22S is a geological epimer, and 22R is a biological epimer [56]. The values of  $C_{29}$  sterane  $\beta\beta/(\beta\beta+\alpha\alpha)$  and  $C_{29}$  sterane 20S/20S+20R for the Sarvak oil samples are in the range of 0.613 to 0.642 and 0.489 to 0.556, respectively, as seen in Table 4. In Figure 12, the variation of  $\beta\beta/(\beta\beta+\alpha\alpha)$  versus 20S/20S+20R in  $C_{29}$  steranes for Sarvak reservoir oil samples in the studied field is shown. As can be seen, all samples represent relatively high maturity. In this diagram, a high-resolution section is obtained where the maturity trend of the Sarvak oil samples can be observed. The lowest maturation is related to well C.

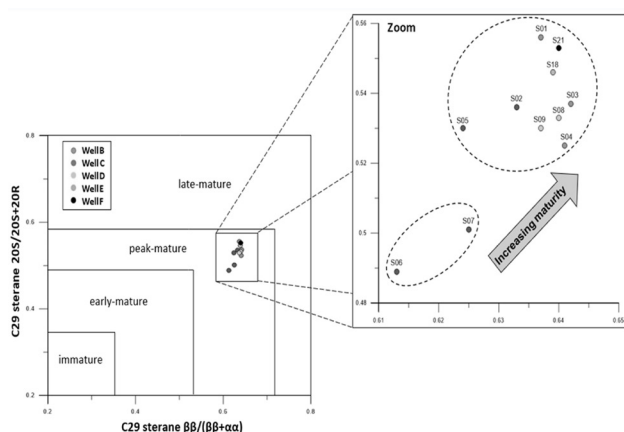


**Fig. 12** Cross-plot of  $C_{29}$  sterane  $\beta\beta/(\beta\beta+\alpha\alpha)$  versus  $C_{29}$  sterane 20S/20S+20R. Determining the thermal maturity range with the Biomarker maturity parameters [57]. A zoomed portion of the figure details the thermal maturity trend of Sarvak reservoir oil samples in the studied field.

Also, the  $C_{32}$  homohopane 22S/(22S+22R) ratios for the Sarvak oil samples are in the range of 0.572 to 0.581, as seen in Table 4. Figure 13 is a cross-plot of  $C_{32}$  homohopane 22S/(22S+22R) versus  $C_{29}$  sterane  $\beta\beta/(\beta\beta+\alpha\alpha)$  that was presented by Peters and Moldowan in 1993 [57]. The plot has been used for the Sarvak reservoir oil samples. As can be seen in this plot, this reservoir's oils indicate the maturity of the peak oil generation stage. Based on this plot, oil samples from well C have the lowest maturity, and well B samples have the highest maturity.

### Possible Origin of the Sarvak Reservoir Oils

So far, the economic accumulation of oil in the Abadan Plain, from the Gadvan and Kazhdumi source rocks, has not been reported [21].

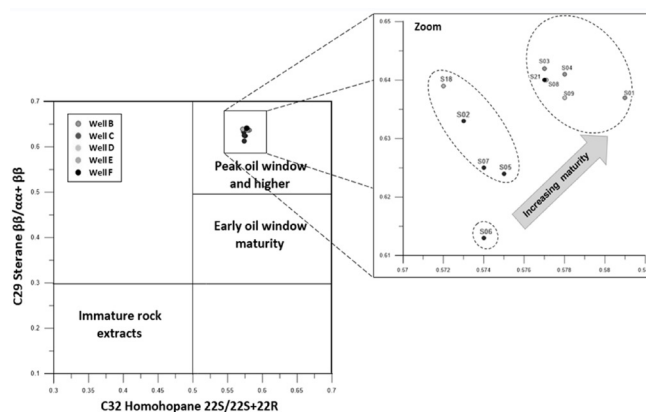


**Fig. 13** Cross-plot of  $C_{29}$  Sterane  $\beta\beta/(\beta\beta+\alpha\alpha)$  versus  $C_{32}$  Homohopanes 22S/(22S+22R) for Sarvak reservoir oil samples [57]. As shown in this figure, the Sarvak reservoir oil samples are in this plot's peak oil window area. In the high-resolution section, the maturity of oils has been shown.

By observing rock-Eval pyrolysis of Kazhdumi Formation in the Abadan Plain, it was found out by Zeinalzadeh et al. in 2018 that this formation has very good TOC contents, and it is fair to good genetic potential. In addition, it was shown that the Kazhdumi Formation with relatively low Tmax and PI is at the thermally immature to early oil generation stage. It is also worth noting that all these parameters are given in Table 7 on average [21].

According to the study which has been carried out by Habibnia et al. in 2015, the variation of S1+S2 and TOC parameters for Kazhdumi Formation has indicated that this formation is assessed as a good source rock for hydrocarbon generation in the Azadegan oilfield. By examining Tmax and HI parameters, it was also shown that this formation has a mixture of type II/III kerogen; therefore, it is not mature enough to generate hydrocarbon. It has not yet entered into the oil generation window [58]. This is largely following the findings of Koraei et al. in 2017 [59]. The values of the mentioned parameters are shown in Table 7 on average.

Therefore, although the Kazhdumi Formation has a good potential for the generation of hydrocarbon in the Abadan Plain, due to insufficient maturity, its role in the high production of hydrocarbon for the Sarvak reservoir is unclear. Elemental analysis results of the Garau and Sargelu formations in the Darquain oilfield (Abadan Plain) reveal 11.6 and 7.4 to 9.6 (average: 8.5) wt.% sulfur content for these formations, respectively, which it allows us to classify these as source rocks containing high-sulfur type II-S kerogen [21,60].

Relatively high values of TOC, HI, and Tmax from the Rock-Eval pyrolysis for the Garau and Sargelu formations (Table 7) classify those as good to excellent potential source rocks with maturity in peak oil generation in the Abadan Plain [16,17,21,61]. All of the above for the Garau and Sargelu formations are consistent with the maturity of peak oil-generative window and high sulfur content (4.6 wt.%) of the Sarvak oil samples in this study.

As can be seen in Table 8, organic geochemical data obtained from the Sarvak reservoir oil samples are almost correlatable with organic geochemical data obtained from the Garau and Sargelu source rocks in most cases.

**Table 7** Some Rock-Eval pyrolysis data related to the Sargelu, Garau, and Kazhdumi formations in the Abadan Plain (all of the values in this table are the average of the data obtained from several samples of each formation) [16,17,18,21,61,58,59].

Formation	Rock-Eval pyrolysis data						
	TOC (%)	S <sub>1</sub> (mg/g)	S <sub>2</sub> (mg/g)	T <sub>max</sub> (°C)	HI (mg/g)	Vr%	PI
Sargelu	1.8	0.84	2.26	445	155	0.80	0.30
Garau	1.6	1.76	4.06	443	220	0.90	0.28
Kazhdumi	2.1	0.57	4.92	429	247	0.57	0.16

TOC: Total Organic Carbon, T<sub>max</sub>: Maximum Temperature, HI: Hydrogen Index, Vr%: Vitrinite reflectance, PI: Production Index (S<sub>2</sub>/S<sub>1</sub>+S<sub>2</sub>)

**Table 8** A comparison between organic geochemical important data related to the Sarvak reservoir oils and Sargelu, Garau, and Kazhdumi source rocks in the Abadan Plain (all of the values in this table are the average of the data obtained from several samples of each formation) [16,17,18,21,62].

Formation	Organic geochemical data (GC and GC-MS)														Vr%
	CPI	TAR	Pr/Ph	Pr/nC <sub>17</sub>	Ph/nC <sub>18</sub>	Ts/ Ts+Tm	G/C <sub>30</sub>	C <sub>32</sub> 22S/R	C <sub>29</sub> 20S/R	C ββ/αα	C <sub>29</sub> /C <sub>30</sub>	δ <sup>13</sup> C Sat(‰)	δ <sup>13</sup> C Aro (‰)	MPI-1	
Sarvak	0.99	0.14	0.65	0.18	0.32	0.16	0.01	0.57	0.53	0.63	1.16	-27.35	-27.75	0.77	0.86
Sargelu	0.98	0.15	0.7	0.42	0.5	0.40	0.02	0.56	0.52	0.58	1.32	-27.27	-26.47	0.74	0.80
Garau	1.04	0.14	0.59	0.47	0.68	0.55	0.11	0.59	0.44	0.53	1.12	-28.40	-28.00	0.71	0.90
Kazhdumi	1.02	-	0.52	0.43	0.54	0.40	-	0.54	0.35	0.37	0.84	-	-	0.70	0.57

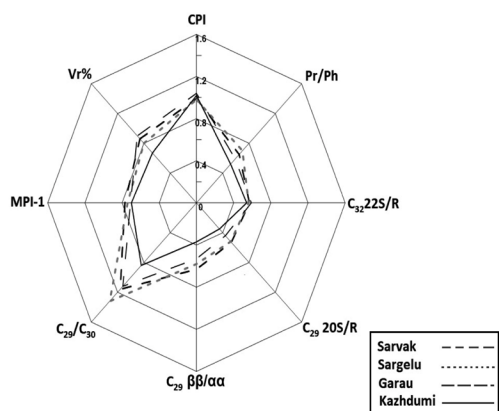
Pr: Pristane, Ph: Phytane,  
G/C<sub>30</sub>: Gammacerane/C30 hopane,  
C<sub>29</sub>/C<sub>30</sub>: C<sub>29</sub>/C<sub>30</sub> hopane,  
C<sub>29</sub> ββ/αα: C<sub>29</sub> Sterane /ββ+αα,  
Sat: Saturate,

Vr%: Vitrinite reflectance,  
Tm: C<sub>27</sub> 17a(H)-22,29,30-trisnorhopane,  
C<sub>32</sub> 22S/R: C<sub>32</sub> Homohopane 22S/22S+22R,  
C<sub>29</sub> 20S/R: C<sub>29</sub> Sterane 20S/20S+20R,  
MPI-1: Methylphenantrene index

Ts: C<sub>27</sub> 18a(H)-22,29,30-trisnorhopane  
TAR: Terrigenous/Aquatic Ratio  
CPI: Carbon Preference Index  
Aro: Aromatic

In Table 8, biomarker maturity parameters (i.e. C<sub>29</sub> ββ/αα, C<sub>29</sub> 20S/R and C<sub>32</sub> 22S/22R) for the Kazhdumi Formation indicate the lower values in comparison with the other formations. It is consistent with the low values of Vr%, T<sub>max</sub>, and PI for this formation in Table 7 (according to Hunt in 1996, by decreasing maturity of organic matter, these parameters will be gradually decreased [28]).

For a better comparison of the organic geochemical data in Table 8, some important parameters in this table were drawn on the star diagram, as seen in Figure 14.

**Fig 14** Star diagram of several important geochemical parameters from Sarvak, Sargelu, Garau, and Kazhdumi formations.

All curves in this diagram show the same trend except the Kazhdumi Formation, with a slight difference from the others.

Therefore, the results of the interpretations and comparisons

made above could largely reflect that the source(s) of the Sarvak reservoir oils in this study could be from the organic-rich parts of the Sargelu and/or Garau formations.

## Conclusions

- In this paper, based on the fractions obtained from the Thin-layer chromatography analysis, it was found out that the composition of all oils from the Sarvak reservoir is mostly naphthenic and paraffinic. Due to the high sulfur content and low API gravity, these oils were considered relatively heavy.
- Using saturated and aromatic biomarker data, carbon isotope ratio (C<sup>13</sup>δ), trace elements (nickel and vanadium), sulfur content (wt.%), and distribution of normal paraffin obtained from gas chromatograms, it was determined that the Sarvak reservoir oils in the study area have a marine-carbonate source rock deposited under anoxic conditions.
- The study of carbon isotope ratios (C<sup>13</sup>δ) represented that the Sarvak oils have a Mesozoic source rock. Also, C<sub>28</sub>/C<sub>29</sub> sterane ratio represents upper Paleozoic and Lower Mesozoic oils. These two pieces of evidence are consistent with the absence of oleanane in Sarvak oils that prove these oils did not derive from upper Cretaceous and Tertiary source rocks.
- The maturation of petroleum was determined by the distribution and frequency of normal paraffin via the gas chromatograms and biomarkers as thermal maturity indicators, including C<sub>29</sub> sterane ββ/(ββ+αα), C<sub>29</sub> sterane 20S/20S+20R, Ts/Ts+Tm trisnorhopane, and C<sub>32</sub> 22S/(22S+22R) homohopanes. The results of this evaluation suggest that all oil samples of the Sarvak reservoir have relatively high maturity.

In this study, the low  $T_s/T_s+T_m$  and diasterane/diasterane + sterane values are mainly due to carbonates in the source rock of the Sarvak reservoir oils, not due to their low maturity.

•Despite the heavy and rich sulfur content of the Sarvak reservoir oils, the oil maturity is relatively high. This indicates a contradiction as the crude oil's thermal maturity increases, the sulfur content decreases, and the API increases. According to the high content of sulfur and the detection of carbonate source rock in this study, this was attributed to the presence of sulfur-rich kerogen (type II-S). However, for taking a closer look at this issue, more data from crude oil are required.

•Based on previous studies, the Garau and Sargelu formations are known as two important source rocks in the Abadan Plain with maturity in the peak oil generation stage and good-excellent hydrocarbon generation potential. Ultimately, comparing the most important organic geochemical data of these two formations with Sarvak oil samples in this study shows that the Sarvak oils are derived probably from organic-rich parts of the Sargelu and/or Garau formations.

### Acknowledgements

We would like to highly express our gratitude to the Institute of Petroleum Engineering (IPE) of University of Tehran for the permission for data publication. We offer special thanks to the Journal of Petroleum Science and Technology (JPST) and anonymous reviewers for their thoughtful and beneficial comments that improved the revised manuscript.

### Nomenclatures

CPI: Carbon preference index

DST: Drill stem test

RFT: Repeat formation test

GC: Gas chromatography

GC-MS: Gas chromatography-mass spectrometry

IR-MS: Isotope-ratio mass spectrometry

TLC-FID: Thin layer chromatography

### References

- Dembicki Jr H (2017) Practical petroleum geochemistry for exploration and production petroleum geochemistry for exploration and production, 1st ed., Elsevier, 1-342.
- Kaufman RL, Ahmed AS, Elsinger RJ (1990) Gas chromatography as a development and production tool for fingerprinting oils from individual reservoirs: Applications in the Gulf of Mexico, Gulf coast oils and gases: Their characteristics, origin, distribution, and exploration and production significance, Proceedings of the 9th Annual Research Conference of the Society of Economic Paleontologists and Mineralogists (SEPM), New Orleans, 263-282.
- Paez RH, Lawrence JJ, Zhang M (2010) Compartmentalization or gravity segregation? Understanding and predicting characteristics of near-critical petroleum fluids, Reservoir compartmentalization, Geological Society, London, Special Publications, 347: 43-53
- Larter S R, Aplin A C (1995) Reservoir geochemistry: methods, applications and opportunities, Geological Society, London, Special Publications, 86: 5-32.
- Bissada KK, Elrod LW, Darnell LM, Szymczyk HM, Trostle JL (1992) Geochemical inversion – a modern approach to inferring source-rock identity from characteristics of accumulated oil and gas. In: Proceedings of the 21st Annual Convention of the Indonesian Petroleum Association, 11: 165–199.
- Peters KE, Walters CC, Moldowan JM (2005) The Biomarker Guide 2: Biomarkers and isotopes in petroleum exploration and earth history, 2nd ed., Cambridge University Press, Cambridge, United Kingdom, 1-471.
- Fuex A (1977) The use of stable carbon isotopes in hydrocarbon exploration, Journal of Geochemical Exploration, 7: 155–188.
- Galimov EM (1975) Carbon isotopes in oil – gas geology, 1st ed., Moscow, Nedra, 1-384.
- Stahl WJ (1979) Carbon isotopes in petroleum geochemistry, In: Lectures in Isotope Geology, 1st ed., Springer-Verlag, New York, 274–223.
- Barwise AJG (1990) Role of nickel and vanadium in petroleum classification, Journal of Energy Fuels, 4: 647-652.
- Alavi M (2004) Regional stratigraphy of the Zagros fold-thrust belt of Iran and its proforeland evolution, American Journal of Science, 304: 1-20.
- Beydoun ZR (1991) Arabian plate hydrocarbon geology and potential-a plate tectonic approach, AAPG Studies in Geology, 33-77.
- Murriss RJ (1980) Middle East: Stratigraphic evolution and oil habitat, AAPG Bulletin, 64: 597-618.
- Zeinalzadeh A, Moussavi-Harami R, Mahboubi A, Sajjadian VA (2015) Basin and petroleum system modeling of the Cretaceous and Jurassic source rocks of the gas and oil reservoirs in Darquain field, south west Iran, Journal of Natural Gas Science and Engineering, 26: 419–426.
- Pitman JK, Steinhauer D, Lewan MD (2004) Petroleum generation and migration in the Mesopotamian Basin and Zagros Fold Belt of Iraq: Results from a basin modeling study, Geo Arabia, 9: 41–72.
- Kobraei M, Rabbani A, Taati F (2019) Upper Jurassic-lower cretaceous source-rock evaluation and oil—source rock correlation in the Abadan plain, Southwest Iran, Geochemistry International, 57, 7: 790–804.
- Kobraei M, Rabbani AR, Taati F (2017) Source rock characteristics of the Early Cretaceous Garau and Gadvan formations in the western Zagros Basin—southwest Iran, Journal of Petroleum Exploration and Production Technology, 7, 4: 1051–1070.
- Kobraei M, Sadouni J, Rabbani AR (2019) Organic geochemical characteristics of Jurassic petroleum system in Abadan Plain and north Dezful zones of the Zagros basin, southwest Iran, Journal of Earth System Science, 128: 1-18.
- Du Y, Chen J, Cui Y, Xin J, Wang J, Li YZ, Fu X (2016) Genetic mechanism and development of the unsteady Sarvak play of the Azadegan oil field, southwest of Iran, Petroleum Science, 13, 1: 34–51.
- Alizadeh B, Saadati H, Rashidi M, Kobraei M (2016) Geochemical investigation of oils from Cretaceous to Eocene sedimentary sequences of the Abadan Plain, Southwest Iran, Marine and Petroleum Geology, 73:

- 609-619.
21. Zeinalzadeh A, Moussavi-Harami R, Mahboubi A, Sajjadian VA (2018) Source rock potential of the Early Cretaceous intervals in the Darquain field, Abadan Plain, Zagros Basin, SW Iran, *Geosciences Journal*, 22: 569-580.
  22. Christian L (1997) Cretaceous Subsurface Geology of the Middle East Region, *GeoArabia*, 2, 3: 239-256.
  23. Setudehnia A (1978) The Mesozoic sequence in southwest Iran and adjacent areas, *Journal of Petroleum Geology*, 1(1): 3-42.
  24. Bordenave ML, Hegre JA (2005) The influence of tectonics on the entrapment of oil in the Dezful Embayment, Zagros Foldbelt, Iranian Journal of Petroleum Geology, 28: 339-368.
  25. Rahimpour-Bonab H, Mehrabi H, Enayati-Bidgoli AH, Omidvar M (2012) Coupled imprints of tropical climate and recurring emergence on reservoir evolution of a middle Cretaceous carbonate ramp, Zagros Basin, southwest Iran, *Cretaceous Research*, 37: 15-34.
  26. Tissot BP, Welte DH (1984) *Petroleum Formation and Occurrence*, 2nd ed., Springer Verlag, Berlin, 1-699.
  27. Baskin DK, Peters KE (1992) Early generation and characteristics of a sulfur-rich Monterey kerogen, *American Association of Petroleum Geologists Bulletin*, 76: 1-13.
  28. Hunt JM (1996) *Petroleum Geochemistry and Geology*, 2nd ed., New York, 1-743.
  29. Waples DW (1985) *Geochemistry in petroleum exploration*, Human Resources Development Corporation, Boston, 1-232.
  30. Bourbonniere RA, Meyers PA (1996) Sedimentary geolipid records of historical changes in the watersheds and productivities of Lakes Ontario and Erie, *Limnology and Oceanography*, 41: 352-359.
  31. Powell TG, McKirdy DM (1973) The effect of source material, rock type and diagenesis on the n-alkane content of sediments, *Geochimistry Cosmochim Acta*, 37: 523 - 633.
  32. Talukdar SC, De Toni B, Marciano F, Sweeney J, Rangel A (1993) Upper Cretaceous source rocks of northern South America, *AAPG Bulletin*, 77, 1-351.
  33. Connan J, Bouroulec J, Dessort D, Albrecht P (1986) The microbial input in carbonate-anhydrite facies of a sabkha palaeoenvironment from Guatemala: a molecular approach, *Organic Geochemistry*, 10: 29-50.
  34. McKirdy DM, Aldridge AK, Ypma PJM (1983) A geochemical comparison of some crude oils from Pre-Ordovician carbonate rocks. In: *Advances in Organic Geochemistry*, Advances in Organic geochemistry, John Wiley and Sons, New York, 99-107.
  35. Moldowan JM, Dahl J, Huizinga BJ, Fago FJ, Hickey LJ, Peakman TM, Taylor DW (1994) The molecular fossil record of oleanane and its relation to the angiosperms, *Science*, 265: 768-771.
  36. Sinninghe Damste JS, Kenig F, Koopmans MP, Sinninghe Damsté JS, Kenig F, Koopmans MP, Koster J, Schouten S, Hayes JM, de Leeuw JW (1995) Evidence for gammacerane as an indicator of water-column stratification, *Geochimica et Cosmochimica Acta*, 59: 1895-900.
  37. Huang WY, Meinschein WG (1979) Sterols as ecological indicators, *Geochim. Cosmochim. Acta*, 43: 739-745.
  38. Mackenzie A, Hoffmann C, Maxwell J (1981) Molecular parameters of maturation in the Toarcian shales, Paris Basin, France—III, Changes in aromatic steroid hydrocarbons, *Geochimica et Cosmochimica Acta*, 45, 8: 1345-1355.
  39. Shanmugam G (1985) Significance of coniferous rain forests and related organic matter in generating commercial quantities of oil, Gippsland Basin, Australia, *AAPG Bulletin*, 69, 8: 1241-1254.
  40. Moldowan JM, Seifert WK, Gallegos EJ (1985) Relationship between petroleum composition and depositional environment of petroleum source rocks, *American association of petroleum geologists--bulletin*, 69: 1255-1268.
  41. Volkman JK (1988) Biological marker compounds as indicators of the depositional environments of petroleum source rocks, *Geological Society, London, Special Publications*, 40, 1: 103-122.
  42. Volkman JK, Barrett SM, Blackburn SI, Mansour MP, Sikes EL, Gelin F (1998) Microalgal biomarkers: a review of recent research developments, *Organic Geochemistry*, 29: 1163-1179.
  43. Shekarifard A, Daryabandeh M, Rashidi M, Hajian M, Röth J (2019) Petroleum geochemical properties of the oil shales from the Early Cretaceous Garau Formation, Qalikh locality, Zagros Mountains, Iran, *International Journal of Coal Geology*, 206: 1-18.
  44. Grantham P J, Wakefield LL (1988) Variations in the sterane carbon number distributions of marine source rock derived crude oils through geological time, *Organic Geochemistry*, 12: 61-73
  45. Lewan M (1984) Factors controlling the proportionality of vanadium to nickel in crude oils, *Geochimica et Cosmochimica Acta*, 48, 11: 2231-2238.
  46. Galarraga F, Reategui K., Martínez A., Martínez M., Llamas J., Márquez G (2008) V/Ni ratio as a parameter in palaeo environmental characterization of nonmature medium-crude oils from several Latin American basins, *Journal of Petroleum Science and Engineering*, 61: 9-14.
  47. Sofer Z (1984) Stable carbon isotope composition of crude oils: Application to source depositional environments and petroleum alteration, *American Association of Petroleum Geologists Bulletin*, 68: 31-49.
  48. Chung HM, Rooney MA, Toon MB, Claypool G. E (1992) Carbon isotope composition of marine crude oils, *AAPG*, 76: 1000-1007.
  49. Bray EE, Evans ED (1965) Hydrocarbons in non-reservoir-rock source beds, *American Association of Petroleum Geologists Bulletin*, 49: 248-257.
  50. Bray EE, Evans ED (1961) Distribution of n-paraffins as a clue to recognition of source beds, *Geochimica et Cosmochimica Acta*, 22: 2-9.
  51. Radke M, Welte DH (1983) The methylphenanthrene index (MPI). A maturity parameter based on aromatic hydrocarbons. In: *Advances in Organic Geochemistry*, John Wiley & Sons, New York, 10: 504-512.
  52. Hughes WB, Holba AG, and Dzou LIP (1995) The ratios of dibenzothiophene to phenanthrene and pristane to

- phytane as indicators of depositional environment and lithology of petroleum source rocks, *Geochimica et Cosmochimica Acta*, 59: 17: 3581–3598.
52. Abay TB, Karlsen DA, Ohm S E (2014) Vertical variations in reservoir geochemistry in a palaeozoic trap, embla field, offshore Norway, *Journal of Petroleum Geology*, 37, 4: 349-372.
  53. Engel MH., Macko SA (1993) *Organic geochemistry*, New York: Plenum Press, 1-861.
  54. Philp RD (1985) *Fossil fuel biomarkers-Application and spectra*, 1st ed., New York: Elsevier, 1-294.
  55. Seifert WK, Moldowan JM (1986) Use of biological markers in petroleum exploration, *Methods in Geochemistry and Geophysics*, 24: 61-290.
  56. Peters KE, Moldowan JM (1993) *The Biomarker guide interpreting molecular fossils in petroleum and ancient sediments*, 1st ed., Englewood Cliffs, NJ, Prentice Hall, 1-363.
  57. Habibnia B, Askari S, Hosseini E, Alizadeh B (2015) Geochemical assessment of Kazhdumi Formation in Azadegan oil field wells using rock-eval pyrolysis, *Journal of Geochemistry*, 4, 3: 231-240 (In Farsi).
  58. Kobraei M, Rabbani AR, Taati F (2017) Investigating Hydrocarbon Generation Potential of Pabdeh (Tertiary) and Kazhdumi (Early Cretaceous) Source Rocks in Abadan Plain, Southwest Iran, *Journal of Petroleum Research*, 27: 4-17 (In Farsi).
  59. Zeinalzadeh A, Moussavi-Harami R, Mahboubi A, Kassaie-Najafi M, Rezaee R (2019) Thermal modelling of gas generation and retention in the Jurassic organic-rich intervals in the Darquain field, Abadan Plain, SW Iran, *Journal of Petroleum Exploration and Production Technology*, 9, 2: 971–987.
  60. Kobraei M and Rabbani A (2018) Gas-condensate potential of the middle-Jurassic petroleum system in Abadan plain, Southwest Iran: Results of 2-D basin modeling, *Energy Sources, Part A: Recovery, Utilization and Environmental Effects*, 40, 10: 1161–1174.
  61. Moradi H, Alizadeh B (2015) Application of detailed molecular maturity parameters in determining thermal maturity of the Kazhdumi Formation in the Yadavaran oil field, *Journal of New Findings in Applied Geology*, 8: 47-57 (In Farsi).